

Results on heavy ion physics at LHCb

Giacomo Graziani, on behalf of the LHCb Collaboration

INFN, Sezione di Firenze

E-mail: Giacomo.Graziani@fi.infn.it

Abstract. In the last years, the LHCb experiment established itself as an important contributor to heavy ion physics by exploiting some of its specific features. Production of particles, notably heavy flavour states, can be studied in p - p , p -Pb and Pb-Pb collisions at LHC energies in the forward rapidity region (pseudorapidity between 2 and 5), providing measurements which are highly complementary to the other LHC experiments. Moreover, owing to its forward geometry, the detector is also well suited to study fixed-target collisions, obtained by impinging the LHC beams on gas targets with different mass numbers. In this configuration, p -A collisions can be studied at the relatively unexplored scale of $\sqrt{s_{NN}} \sim 100$ GeV, also providing valuable inputs to cosmic ray physics. An overview of the measurements obtained so far by the LHCb ion program is presented.

1. Introduction

The LHCb experiment [1] has been conceived with the main goal of studying heavy flavour physics in p - p collisions at the LHC, exploiting the unprecedented yield of b -quark pairs, which are mainly produced at small angles with respect to the direction of the colliding proton beams. The detector is therefore designed as a forward spectrometer covering the pseudorapidity region $2 < \eta < 5$ and providing excellent vertexing, tracking and particle identification capabilities for the reconstruction of heavy flavour decays. Another key feature is the online selection system, consisting of a hardware level with high output bandwidth (up to 1 MHz), followed by a software level providing high flexibility.

Though heavy ion physics was not among the original motivations for the experiment, the detector capabilities offer some unique possibilities also for this field:

- the forward acceptance, with a fully instrumented detector, highly complementary to the other LHC experiments;
- the excellent reconstruction performance, unrivaled at the LHC, for exclusive heavy flavour states down to null transverse momentum (p_T), disentangling charmed particles produced promptly from those coming from b -hadron decays;
- the possibility to operate the detector in fixed target mode, by injecting small amount of noble gas (He, Ne and Ar) in the LHC vacuum [2] and studying beam-gas collisions, for which the forward geometry of the detector is very well suited.

On the other hand, the most central Pb-Pb collisions can't be properly reconstructed due to the high track density in the forward region. LHCb is therefore more suited for smaller collision systems like p -Pb, but can contribute also to study peripheral Pb-Pb collisions. It has to be noted that studies in small collision systems have become increasingly important to the

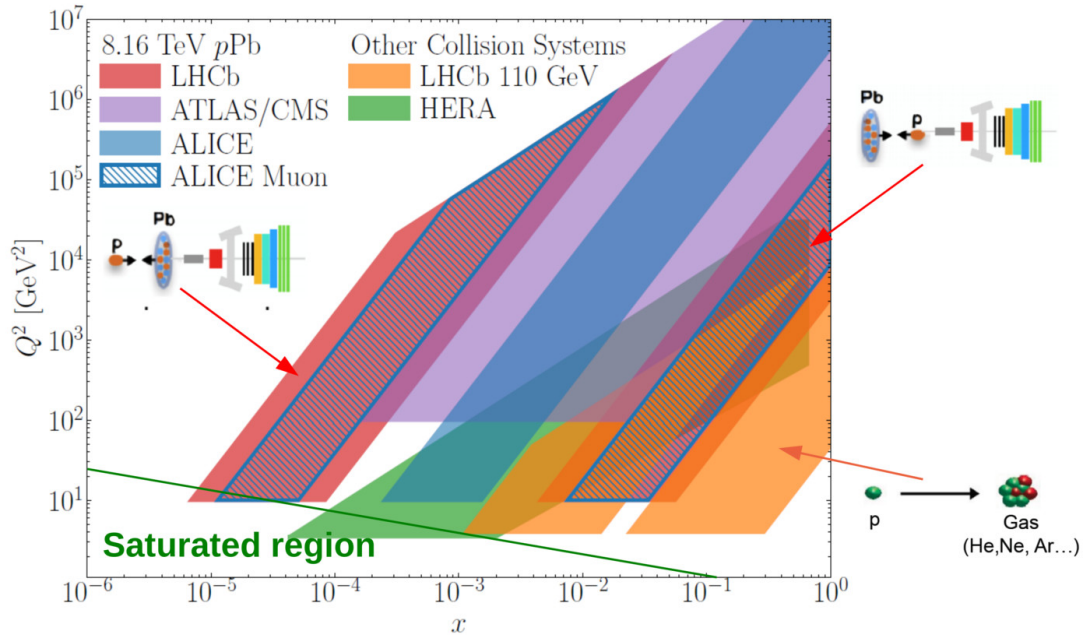


Figure 1. Kinematic reach corresponding to the acceptance of the four LHC experiments in p -Pb collisions. The kinematic regions accessible in the fixed-target configuration at LHCb and in e - p collisions at HERA are also shown.

interpretation of relativistic heavy ion collisions after the discovery, performed at the LHC, of sizeable collective behaviour even in p - p collisions [3].

A comparison among the kinematic reaches of LHCb and the other LHC experiments in p - A collisions, in terms of the Bjorken- x value of the nucleon in the nuclear target and the squared parton-parton invariant mass Q^2 , is shown in Figure 1. Two regions are covered in p -Pb collisions, depending on the orientation of the proton and lead beams. The so-called *forward* configuration, when the proton beam points toward the detector (i.e., it enters the detector region from its vertex detector), corresponds to values of x down to 10^{-5} , where gluon saturation is expected to occur. In the *backward* configuration, when the Pb beam points toward the detector, measurements are sensitive to the anti-shadowing region up to $x \sim 0.1$.

In fixed target collisions, the nucleon-nucleon centre-of-mass (c.m.) energy reaches 110 GeV for proton beams of 6.5 TeV energy. Measurements at this energy scale, intermediate between SPS fixed target experiments and beam-beam collisions at LHC, provides an additional test bed to explore the energy evolution in the dynamics of nuclear matter. The detector acceptance corresponds to mid and backward rapidities in the c.m. frame: $-2.8 < y^* < 0.2$. As also depicted in Figure 1, this gives access to large values of x in the target nucleon, where nuclear PDFs are modified by the EMC effect and where the contribution of a possible intrinsic heavy quark content in the nucleon could be substantiated.

2. p -Pb collisions

The experiment collected a first dataset of p -Pb collisions at $\sqrt{s_{NN}} = 5.02$ TeV in 2013, corresponding to integrated luminosities of 1.1 and 0.5 nb^{-1} in the forward and backward configuration, respectively. After this successful experience, larger luminosities were delivered to LHCb during the 2016 p -Pb run at $\sqrt{s_{NN}} = 8.16$ TeV, with 13.6 and 30.8 nb^{-1} recorded. The results published so far by LHCb focus on production of heavy flavour states, whose modification

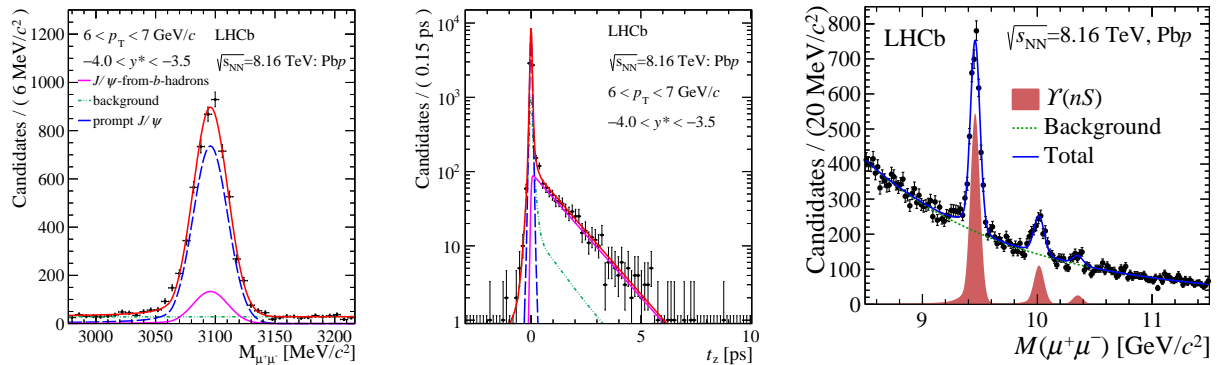


Figure 2. Distributions of (left) reconstructed mass and (middle) pseudo-proper time $t_z \equiv (z_{J/\psi} - z_{PV}) \times (M/p_z)_{J/\psi}$ for the $J/\psi \rightarrow \mu^+\mu^-$ decay candidates from the 8 TeV Pb- p sample [4] in the rapidity bin $-4.0 < y^* < -3.5$ ($z_{J/\psi}$ and z_{PV} are the reconstructed longitudinal position of the J/ψ decay vertex and the interaction primary vertex, respectively). The result of a fit to determine prompt signal, from- b signal and background fractions is overdrawn. In the right plot, mass distribution for the $\Upsilon(nS)$ candidates from the same sample in $-5.0 < y^* < -2.5$ [5].

with respect to p - p collisions constitutes a major probe for the hot and dense matter, known as quark-gluon plasma (QGP), produced in Pb-Pb collisions at LHC. In p -Pb collisions QGP is not expected to be formed and the system is considered to be a reference for the understanding of cold nuclear matter (CNM) effects.

Figure 2 illustrates the ability to distinguish promptly produced J/ψ mesons from those produced in b -hadron decays in reconstructed $J/\psi \rightarrow \mu^+\mu^-$ decays. The nuclear modification factor $R_{pPb} \equiv \sigma_{pPb}/(A_{Pb} \sigma_{pp})$, where σ_{pPb} and σ_{pp} are the production cross-sections in the two collision systems and $A_{Pb} = 208$ is the lead mass number, can be measured separately for the two components. The result for the prompt component obtained from the 8 TeV sample [4] is shown in Figure 3 as a function of p_T and the c.m. rapidity y^* . A clear suppression with respect to p - p collisions is observed at forward rapidity and low p_T , compatible with the expected effect from nuclear PDF modifications (shadowing) as computed in the framework of NRQCD factorisation using several collinear nuclear PDF sets with the HELAC-Onia package [6, 7]. However, the rapidity dependence can also be well explained by the coherent energy loss model [8]. The result at forward rapidity is also compatible with the latest calculations based on the Color Glass Condensate model [9]. More measurements, notably on Drell-Yan production, are needed to disentangle these physical effects [10].

If final-state effects in CNM can't be excluded from the J/ψ result, they are definitely needed to explain the different modifications of quarkonia states. The first measurement of $\psi(2S)$ production in the 5 TeV sample [11] indicated a larger suppression with respect to J/ψ , in agreement with results from the other LHC experiments [12–15]. A more recent result [5] shows evidence for different suppression among the three $\Upsilon(nS)$ states, which are cleanly observed in the 8 TeV sample (see Figure 2). The result, shown in Figure 4, is nicely described in the framework of the “comovers” model [16], where dissociation of the quarkonia states is attributed to interaction with final-state particles which are close in phase-space. This relatively large effect needs to be taken into account in the interpretation of the spectacular suppression of Υ states recently observed by CMS in Pb-Pb collisions [17].

Production of open charm states, D^0 mesons [18] and Λ_c^+ baryons [19], has also been measured with large statistics already in the 5 TeV sample. Data are precise enough to constrain nuclear PDFs, assuming that initial-state effects dominate the observed nuclear modification.

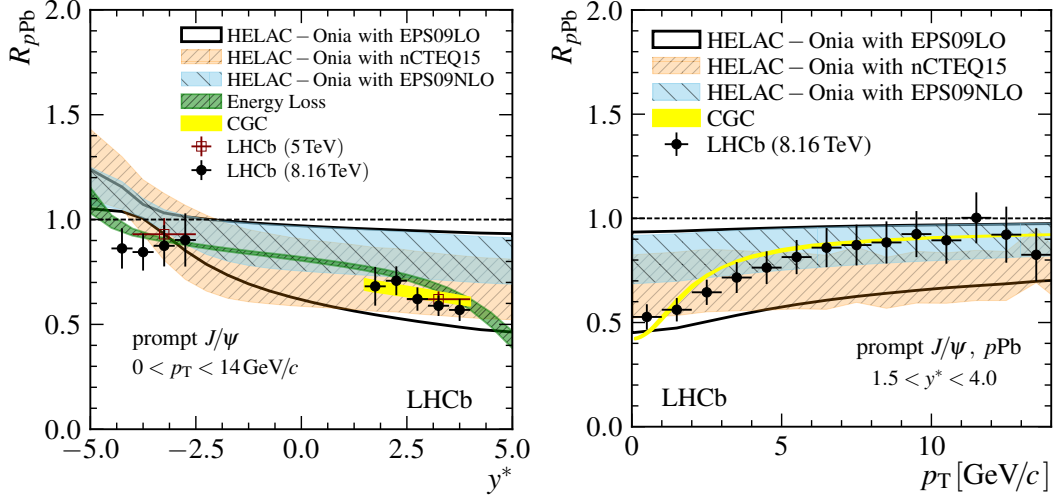


Figure 3. Nuclear modification factor R_{pPb} for prompt J/ψ production as a function of (left plot) y^* and (right plot) p_T for the forward configuration [4].

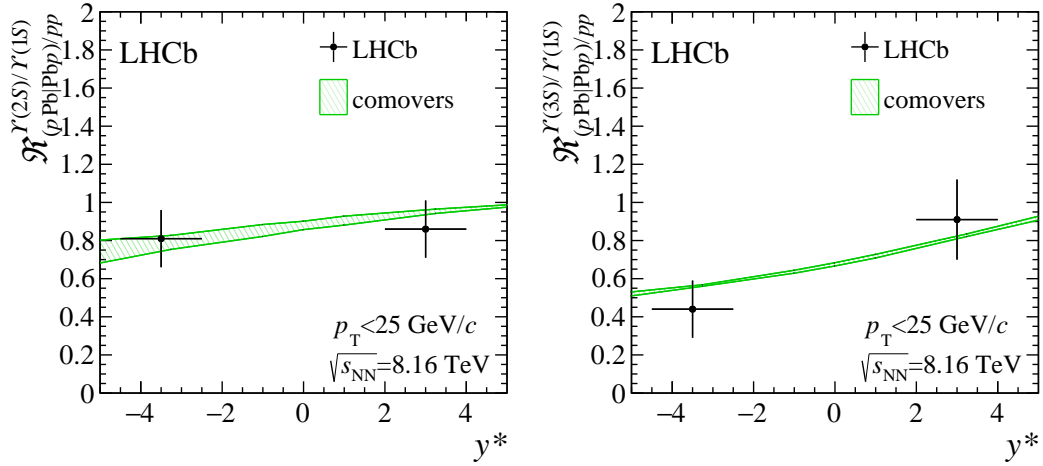


Figure 4. Ratio between Υ nuclear modification factors as a function of rapidity for (left plot) $\Upsilon(2S)/\Upsilon(1S)$ and (right plot) $\Upsilon(3S)/\Upsilon(1S)$ [5].

The Λ_c^+/D^0 ratio is an important input to the hadronisation phenomenology, since baryon enhancement in heavy ion collisions, notably at low p_T , is expected from production via coalescence and is affected by the thermal properties of the nuclear medium. LHCb measures a ratio between the Λ_c^+ and D^0 prompt production around 0.3, with no evidence of strong dependence on the rapidity or transverse momentum (see Figure 5). Results are in substantial agreement with HELAC-onia computations where the only nuclear effects are due to PDF modifications and largely cancel in the ratio.

For the first time, exclusive b -hadron decays have been reconstructed in nuclear collisions [21]. Clean samples of four decay modes ($B^+ \rightarrow \bar{D}^0\pi^+$, $B^+ \rightarrow J/\psi K^+$, $B^0 \rightarrow D^-\pi^+$, $\Lambda_b^0 \rightarrow \Lambda_c^+\pi^-$) have been obtained from the 8 TeV p -Pb dataset, down to p_T values below the hadron mass. The B^+ modes have been used to measure the nuclear modification factor as a function of y^* and p_T . The results, shown in Figure 6, confirm the suppression pattern observed with detached J/ψ , consistently with nuclear PDF effects. The ratio between prompt production of Λ_b^0 baryons

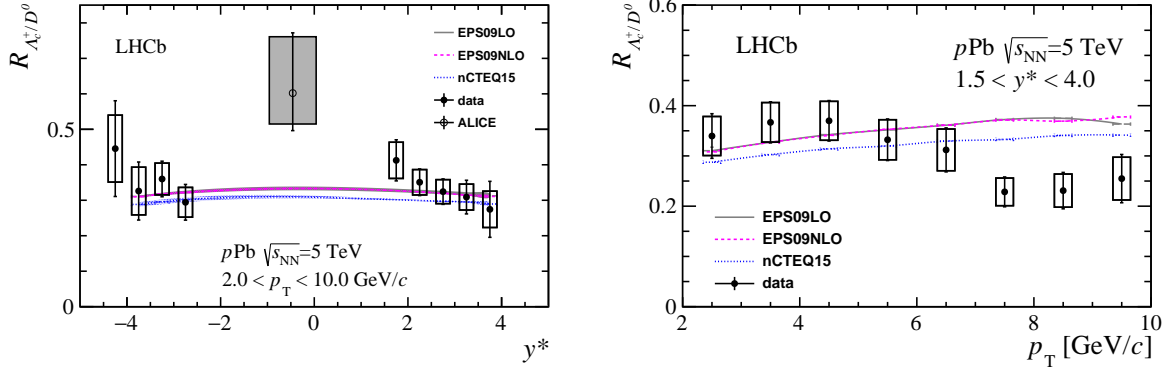


Figure 5. Ratio between Λ_c^+ and D^0 production in p -Pb collisions at 5 TeV, as a function of (left plot) y^* and (right plot) p_T for the forward configuration [19]. The result from ALICE [20] at mid rapidities is also shown for comparison.

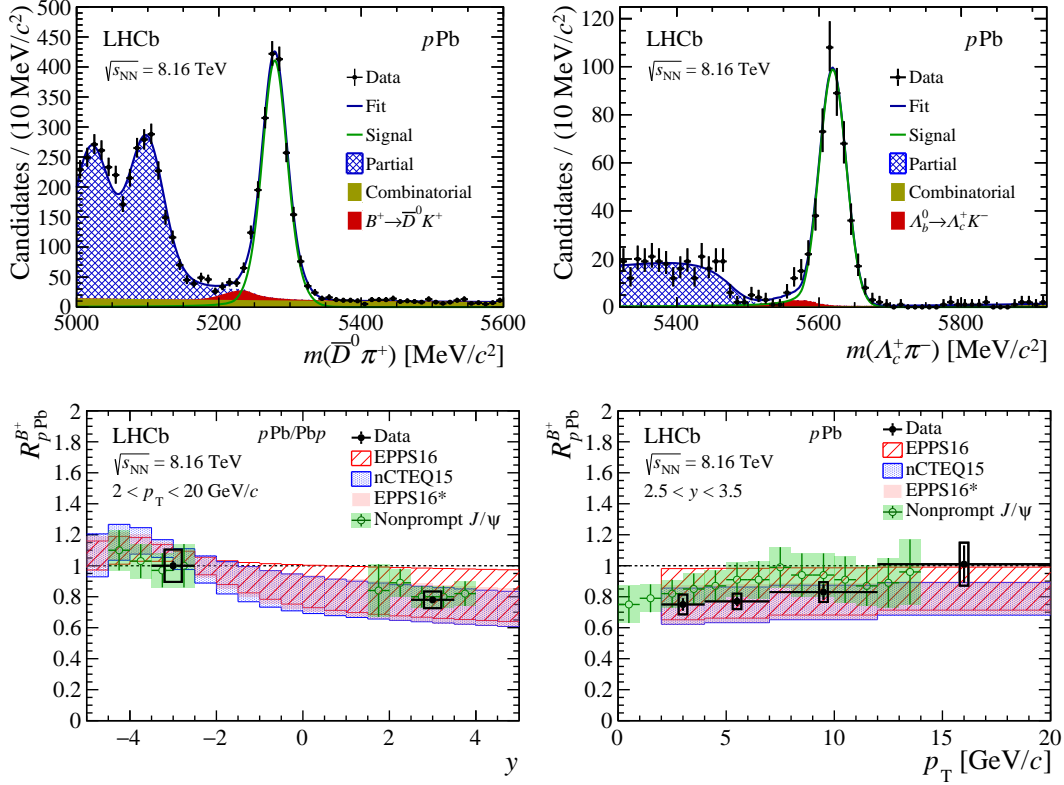


Figure 6. In the upper plots, reconstructed mass distribution of candidates for the (left) $B^+ \rightarrow \bar{D}^0 \pi^+$ and (right) $\Lambda_b^0 \rightarrow \Lambda_c^+ \pi^-$ decays in the p -Pb forward configuration data at 8 TeV. In the lower plots, the resulting nuclear modification factor R_{pPb} for B^+ meson production is plotted as a function of (left plot) y^* and (right plot) p_T for the forward configuration [21]. Results are compared with the measurement for J/ψ from b -hadron decays [4] and with HELAC-onia calculations using different nuclear PDF sets.

and B^0 mesons is also measured and found consistent with the p - p measurement.

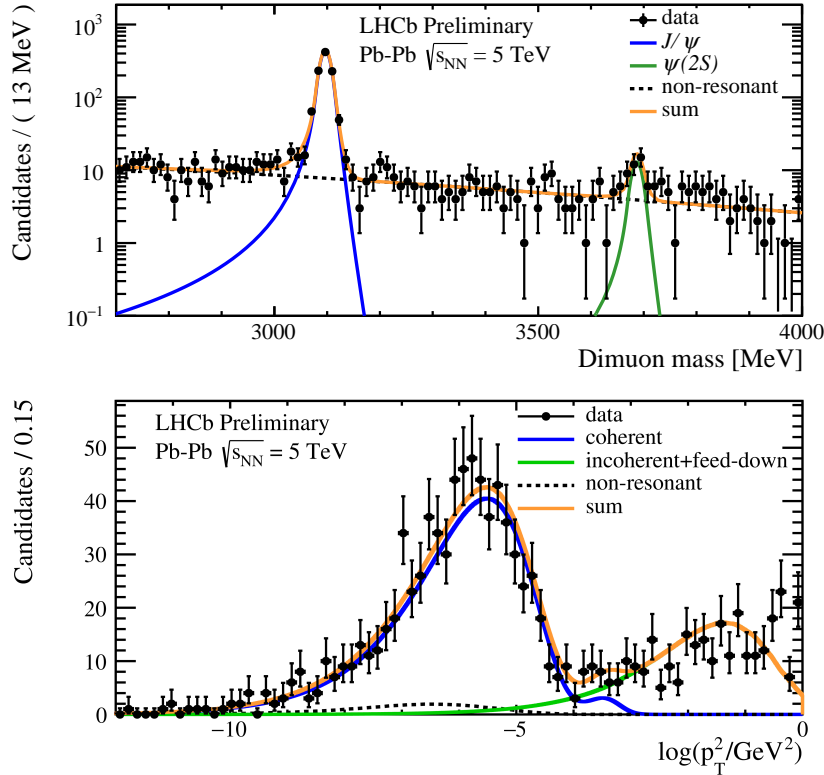


Figure 7. Candidates for J/ψ exclusive production in Pb-Pb collisions at 5 TeV [22], reconstructed from $J/\psi \rightarrow \mu^+\mu^-$ decays. In the upper plot, the reconstructed mass distribution is shown in an extended mass range where, beside the clean J/ψ peak, a small signal for $\psi(2S)$ can also be seen. In the lower plot, the $\log(p_T^2)$ distribution in the J/ψ mass range (3096.9 ± 65 MeV) is fitted with templates for coherent and incoherent production.

3. Pb-Pb collisions

A first small sample of Pb-Pb collisions was recorded by LHCb during the 2015 run, corresponding to about $10 \mu\text{b}^{-1}$. The tracking detector performance in this challenging environment was found to be satisfactory for events of centrality above 50%.

The first preliminary physics result [22] has been obtained from ultraperipheral collisions (UPC), where hadron photoproduction is enhanced by the large photon flux from the lead nuclei. The observation of photoproduction of heavy flavour states, providing a hard scale for perturbative QCD calculations, is particularly interesting to explore the gluon density down to the saturation region at $x \sim 10^{-5}$. The exclusive production of J/ψ is cleanly observed (see Figure 7). The excellent p_T resolution allows to distinguish coherent and incoherent production, whose p_T distributions are found to be well described by templates obtained with the STARlight generator [23].

The accuracy of the result is limited by the size of the data sample, but this analysis demonstrates the LHCb potential for physics in Pb-Pb UPC. During the run performed in november 2018, an integrated luminosity of $210 \mu\text{b}^{-1}$ was collected, providing the possibility for a precision measurement of exclusive J/ψ and $\psi(2S)$ production, and possibly to access rarer channels like Υ production and light-by-light scattering.

4. Fixed-target collisions

Samples of beam-gas collisions with proton and lead beams of different energy, and with the three possible targets (He, Ne and Ar) have been collected by LHCb during the LHC Run 2, as summarized in Figure 8. The largest sample, p -Ne collisions at $\sqrt{s_{NN}} = 69$ GeV, corresponds to an integrated luminosity of about 100 nb^{-1} . A sample of Pb-Ne collisions at the same energy has been recently collected during the 2018 Pb-Pb run.

The first physics results, demonstrating the potential of this novel program, have been obtained from some of the first samples collected in 2015 and 2016. The first measurement of charm production [24] is based on the $7.6 \pm 0.5 \text{ nb}^{-1}$ of p -He collisions at 87 GeV, and a few nb^{-1} of p -Ar data at 110 GeV. Order of 10^3 D^0 mesons and 10^2 J/ψ mesons are reconstructed from both samples. These data provide the first determination of the $c\bar{c}$ cross-section at this relatively unexplored energy scale (see Figure 9). The rapidity dependence of the production is found to agree with predictions based on collinear factorisation not including a contribution from intrinsic charm, as shown in Figure 9. Therefore, these measurements, which are sensitive to x values up to ~ 0.5 , do not favour the large intrinsic charm contributions predicted by some models in this kinematic range [25, 26]. The larger available datasets, and possibly the use of a hydrogen target in the future, will allow for more accurate constraints.

The antiproton production in the p -He sample at 110 GeV [28] has also been measured. This study is motivated by the recent precision measurements performed in space, notably by AMS-02 [29], of the antiproton content in cosmic rays, which is sensitive to possible exotic contributions like dark matter annihilation. For antiprotons above 10 GeV, the largest uncertainty on the expected flux of antiprotons from known sources, namely production in collisions between primary cosmic rays and the interstellar medium, is due to the limited knowledge of the corresponding production cross-sections. LHCb performed the first \bar{p} production measurement in p -He collisions, which are responsible for about 40% of the expected cosmic \bar{p} flux, in the range of \bar{p} momentum between 12 and 110 GeV. The results, shown in Figure 10, are significantly more precise than the spread among the predictions from different phenomenological models,

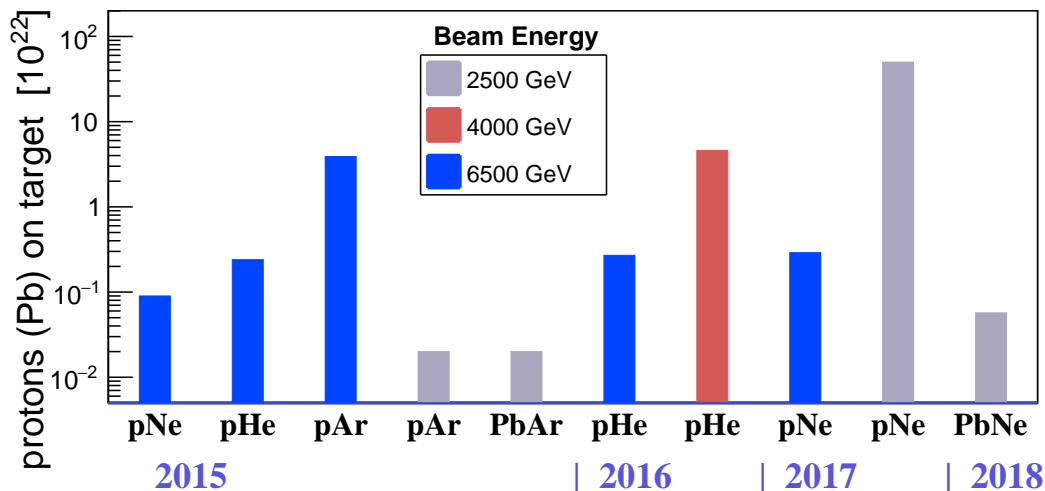


Figure 8. Summary of collected fixed-target physics samples at LHCb. The data size is given in terms of delivered protons (ions) on target (POT). For a nominal target pressure of 2×10^{-7} mbar, 10^{22} POT correspond to an integrated luminosity of about 5 nb^{-1} per meter of gas, though the actual target pressure and the data taking efficiency vary among samples.

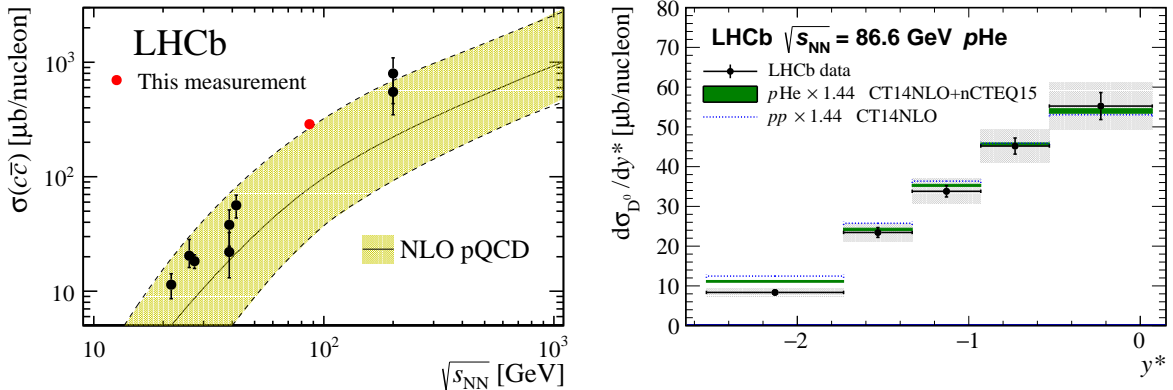


Figure 9. In the left plot, the result for the $c\bar{c}$ production cross-section per nucleon, obtained from p -He collisions at 69 GeV [24], is compared with other experimental results and with a NRQCD calculation [27]. The right plot shows the rapidity dependence of the D^0 production cross-section in the same sample. The result is compared with HELAC-onia calculations, not accounting for intrinsic charm, which are rescaled to reproduce the integrated value of the measured cross-section.

and are contributing to improve the models for cosmic secondary \bar{p} and the resulting constraints on dark matter contributions [30, 31].

For both results, the integrated luminosity of the sample is estimated from the yield of elastically scattered electrons from the target atoms. The yield is determined by selecting events with a single low-pt track in the detector, identified as an e^\pm . The background to this normalization channel is due to soft diffractive collisions with a single track reconstructed in the detector and is expected to be symmetric in charge, so that it can be estimated and subtracted using the e^+ candidates, as illustrated in Figure 10. The integrated luminosity is determined using this method with an accuracy of 6% [28], dominated by the systematic uncertainty on the electron reconstruction efficiency.

5. Conclusions and Prospects

The results obtained so far by the LHCb collaboration from heavy ion collisions demonstrate the capability of the experiment to provide unique contributions to this field, exploiting a variety of collision systems and energy scales, where exclusive final states, notably in the heavy flavour sector, can be reconstructed with high efficiency and purity.

The rich datasets collected so far provide many additional possibilities that are being investigated. In p -Pb collisions, studies on direct photons, both inclusive and in gamma-jet events, are underway, with unique sensitivity to the saturation region [33]. The size of the sample collected in 2018 at 8 TeV is expected to provide access to new channels, as χ_c and η_c quarkonia states and Drell-Yan dimuon events. Studies of flow and correlations with identified particles in the unique forward acceptance region covered by LHCb are also planned.

Substantial development of the heavy ion program in LHCb is also expected during the future LHC runs, taking profit of the currently ongoing detector upgrade [34] which includes a new vertex detector with improved granularity. The proposed plans for future heavy ion running, discussed in detail in Reference [35], foresee an increase in integrated luminosity for p -Pb and Pb-Pb collisions by more than an order of magnitude during the LHC Runs 3 and 4 (2021-2029). This will open novel possibilities, as precision studies using Drell-Yan events and correlations in heavy flavour production. A proposal for a second detector upgrade for the LHC Run 5 (starting 2031) has been put forward [36, 37]. The granularity of such detector, conceived to take profit

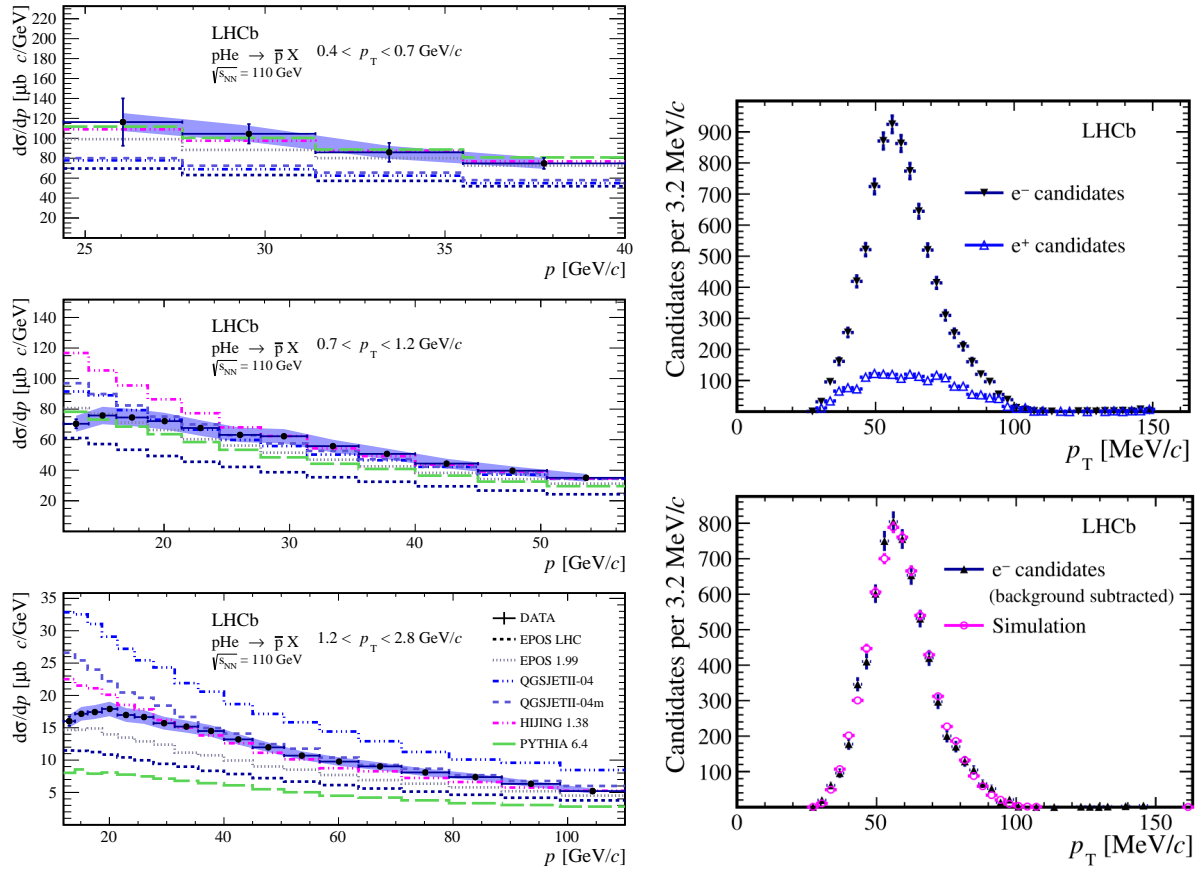


Figure 10. On the left plot, result for antiproton production in p -He collisions at 110 GeV. The differential production cross-section $d\sigma/dp$ is shown as a function of the momentum p for different ranges of p_T and is compared with several generators included in the CRMC package [32]. The normalization is obtained from the p - e^- elastic scattering events from the same sample, illustrated in the right plots. The upper plot shows the p_T distribution for single scattered electron candidates with negative and positive charge, the latter sample being used to subtract the background from hadronic collisions. After subtraction, the distribution is found to agree well with the expected one from simulated p - e^- scattering, as shown in the lower plot.

of the full potential of LHC luminosity in p - p collisions, would make it possible to reconstruct even the most central Pb-Pb collisions.

The fixed-target program will also be considerably developed, thanks to the installation of a new target device [38]. This will consist of a storage cell containing the injected gas into a 20 cm long region located just upstream the LHCb vertex detector. An increase in fixed-target luminosity by up to two orders of magnitude with the same injected gas flow is anticipated. Furthermore, it will be possible to inject more gas species, notably hydrogen, providing p - p reference for the other fixed-target samples. The physics potential of such program, discussed in more detail in Reference [39], covers a wealth of measurements that won't be possible at any other facility in the coming years, including heavy flavour and Drell-Yan production giving access to nuclear PDFs at large x , measurements of quarkonia suppression in different systems at $\sqrt{s_{NN}} \sim 100$ GeV, and studies of particle production of great interest for cosmic ray physics.

References

- [1] Alves Jr A A *et al.* (LHCb collaboration) 2008 *JINST* **3** S08005
- [2] Barschel C 2014 Ph.D. thesis RWTH Aachen U. CERN-THESIS-2013-301
- [3] Khachatryan V *et al.* (CMS collaboration) 2010 *JHEP* **09** 091 (*Preprint* 1009.4122)
- [4] Aaij R *et al.* (LHCb collaboration) 2017 *Phys. Lett.* **B774** 159 (*Preprint* 1706.07122)
- [5] Aaij R *et al.* (LHCb collaboration) 2018 *JHEP* **11** 194 (*Preprint* 1810.07655)
- [6] Shao H S 2016 *Comput. Phys. Commun.* **198** 238–259 (*Preprint* 1507.03435)
- [7] Lansberg J P and Shao H S 2017 *Eur. Phys. J.* **C77** 1 (*Preprint* 1610.05382)
- [8] Arleo F and Peigné S 2013 *JHEP* **03** 122 (*Preprint* 1212.0434)
- [9] Duclou B, Lappi T and Mntysaari H 2016 *Phys. Rev.* **D94** 074031 (*Preprint* 1605.05680)
- [10] Arleo F and Peign S 2017 *Phys. Rev.* **D95** 011502 (*Preprint* 1512.01794)
- [11] Aaij R *et al.* (LHCb collaboration) 2016 *JHEP* **03** 133 (*Preprint* 1601.07878)
- [12] Abelev B B *et al.* (ALICE collaboration) 2014 *JHEP* **12** 073 (*Preprint* 1405.3796)
- [13] Adam J *et al.* (ALICE collaboration) 2016 *JHEP* **06** 050 (*Preprint* 1603.02816)
- [14] Aaboud M *et al.* (ATLAS collaboration) 2018 *Eur. Phys. J.* **C78** 171 (*Preprint* 1709.03089)
- [15] Sirunyan A M *et al.* (CMS collaboration) 2019 *Phys. Lett.* **B790** 509–532 (*Preprint* 1805.02248)
- [16] Ferreiro E G and Lansberg J P 2018 *JHEP* **10** 094 [Erratum: *JHEP*03,063(2019)] (*Preprint* 1804.04474)
- [17] Sirunyan A M *et al.* (CMS collaboration) 2019 *Phys. Lett.* **B790** 270–293 (*Preprint* 1805.09215)
- [18] Aaij R *et al.* (LHCb collaboration) 2017 *JHEP* **10** 090 (*Preprint* 1707.02750)
- [19] Aaij R *et al.* (LHCb collaboration) 2019 *JHEP* **02** 102 (*Preprint* 1809.01404)
- [20] Acharya S *et al.* (ALICE collaboration) 2018 *JHEP* **04** 108 (*Preprint* 1712.09581)
- [21] Aaij R *et al.* (LHCb collaboration) 2019 *Phys. Rev.* **D99** 052011 (*Preprint* 1902.05599)
- [22] LHCb collaboration 2018 LHCb–CONF–2018–003
- [23] Klein S R, Nystrand J, Seger J, Gorbunov Y and Butterworth J 2017 *Comput. Phys. Commun.* **212** 258–268 (*Preprint* 1607.03838)
- [24] Aaij R *et al.* (LHCb collaboration) 2018 *Phys. Rev. Lett.* **122** 132002 (*Preprint* 1810.07907)
- [25] Pumplin J, Lai H L and Tung W K 2007 *Phys. Rev.* **D75** 054029 (*Preprint* hep-ph/0701220)
- [26] Brodsky S J, Kusina A, Lyonnet F, Schienbein I, Spiesberger H and Vogt R 2015 *Adv. High Energy Phys.* **2015** 231547 (*Preprint* 1504.06287)
- [27] Maltoni F *et al.* 2006 *Phys. Lett.* **B638** 202–208 (*Preprint* hep-ph/0601203)
- [28] Aaij R *et al.* (LHCb collaboration) 2018 *Phys. Rev. Lett.* **121** 222001 (*Preprint* 1808.06127)
- [29] Kounine A 2012 *Int. J. Mod. Phys.* **E21** 1230005
- [30] Reinert A and Winkler M W 2018 *JCAP* **1801** 055 (*Preprint* 1712.00002)
- [31] Korsmeier M, Donato F and Di Mauro M 2018 *Phys. Rev. D* **97**(10) 103019 (*Preprint* 1802.03030)
- [32] Pierog T, Baus C and Ulrich R CRMC (Cosmic Ray Monte Carlo package) web.ikp.kit.edu/rulrich/crmc.html
- [33] Da Silva C (LHCb collaboration) 2018 Contribution to the Quark Matter 2018 conference URL <https://indico.cern.ch/event/656452/contributions/2859624>
- [34] LHCb collaboration 2012
- [35] Citron Z *et al.* 2018 *HL/HE-LHC Workshop Report* (*Preprint* 1812.06772)
- [36] LHCb collaboration 2017 CERN–LHCC–2017–003
- [37] LHCb collaboration 2018 CERN–LHCC–2018–027 LHCb–PUB–2018–009 (*Preprint* 1808.08865)
- [38] Di Nezza P *et al.* 2018 Tech. Rep. CERN-PBC-Notes-2018-007
- [39] Graziani G *et al.* 2018 Tech. Rep. LHCb-PUB-2018-015